# Some challenges in the first-principles modeling of structures and processes in electrochemical energy storage and transfer

Nicolas G. Hörmann[1,2], Markus Jäckle[1,2], Florian Gossenberger[2], Tanglaw Roman[2], Katrin Forster-Tonigold[1], Maryam Naderian[2], Sung Sakong[2], and Axel Groß[1,2]
[1] *Helmholtz Institute Ulm (HIU) Electrochemical Energy Storage, Albert-Einstein-Allee 11, 89069 Ulm/Germany*
[2] *University of Ulm, Institute of Theoretical Chemistry, Albert-Einstein-Allee 11, 89069 Ulm/Germany*

In spite of the strong relevance of electrochemical energy conversion and storage, the atomistic modeling of structures and processes in electrochemical systems from first principles is hampered by severe problems. Among others, these problems are associated with the theoretical description of the electrode potential, the characterization of interfaces, the proper treatment of liquid electrolytes, changes in the bulk structure of battery electrodes, and limitations of the functionals used in first-principles electronic structure calculations. We will illustrate these obstacles, but also indicate strategies to overcome them.

## I. INTRODUCTION

In spite of its technological relevance in the electrochemical energy conversion and storage, our knowledge about the microscopic structure of devices, in particular at electrode/electrolyte interfaces is still limited [1]. This is among others caused by the fact that the experimental determination of bulk and interface structures is not trivial. Here simulations on the microscopic level together with a multi-scale modeling approach could be rather helpful.

However, the atomistic theoretical description of these structures is hampered by several facts. i) Electrochemical interfaces, in particular in batteries, are often very poorly characterized since experimental tools with atomic resolution often do not work at these interfaces. This makes the theoretical structure determination difficult as hardly any experimental information can be used as input. ii) Liquid electrolytes require to determine free energies instead of just total energies. This means that computationally expensive statistical averages have to be performed [2, 3]. iii) In electrochemistry, structures and properties of the electrode-electrolyte interfaces are governed by the electrode potential which adds considerable complexity to the theoretical treatment since charged interfaces need to be considered [4–8]. iv) Upon charging and discharging, significant structural changes can occur in the electrodes, realized as volume changes or phase transitions [9]. These can not be properly handled by atomistic techniques alone, but require the combination of atomistic modeling with a continuum description. v) As far as first-principles approaches are concerned, electronic structure methods based on density functional theory (DFT) combine numerical efficiency with satisfactory accuracy for a wide class of systems and materials [10]. However, this is not true for all materials used as electrodes or electrolytes in electrochemical storage and conversion.

It is fair to say that despite these obstacles, significant progress has already been made in the atomistic modeling of devices in electrochemical storage and conversion [11]. It is furthermore evident that nowadays computational modeling is an integral part of research and development in materials and interface sciences [10, 12]. Still, in this contribution we will illustrate some of the challenges in the atomistic modeling of electrochemical storage and conversion devices, but also indicate possible strategies to handle these obstacles. We will mainly concentrate on interface issues at the electrochemical boundary between electrode and electrolyte, in particular with respect to the structure and composition of these interfaces, but we will also discuss issues associated with the volume change upon charging and discharging in batteries.

## II. COMPUTATIONAL DETAILS

The periodic density functional theory calculations presented in this paper have been performed using the Vienna ab initio simulation package (VASP) [13]. Electron-core interactions were accounted for by the projector augmented wave method [14, 15]. Typically the functional of Perdew, Burke, and Ernzerhof (PBE) [16] was employed in the Generalized Gradient Approximation (GGA) in order to describe the exchange-correlation effects. The electronic one-particle wave functions were expanded in a plane-wave basis set up using a sufficiently high energy cutoff of at least 400 eV. The convergence of the results with respect to the k-point set was carefully monitored. In the surface calculations, at least the uppermost two layers were allowed to relax.

## III. STRUCTURE OF INTERFACES IN ELECTROCHEMICAL STORAGE AND CONVERSION DEVICES

### A. Thermodynamic approach to model the presence of electrolytes at interfaces

As far as the interfaces between electrodes and electrolytes are concerned, it is important to note that the presence of the electrolyte has a significant influence on the surface structure of the electrode. Now in particular

in batteries these interfaces can be rather complex. The classical example is the solid electrolyte interphase (SEI) that forms at negative battery electrodes.

Modeling the SEI atomistically represents a significant challenge. Because of its complexity, first-principles studies are limited to the initial stages of SEI formation [17–20] which are assumed to be due to the decomposition of the electrolyte such as ethylene carbonate (EC) [21]. Ion transport through the SEI can hardly be modeled on a first-principles basis, but it can be adressed on a force-field level [22]. For example, MD simulations of the $Li^+$ transport through the dilithium ethylene dicarbonate (Li2EDC) component of the SEI yielded activation energies for $Li^+$ diffusion and conductivity in good agreement with experiment [23].

Still, it is desirable to address electrode properties by electronic structure calculations inspired by the applicability of traditional surface science approaches for electrochemistry surfaces [7, 24]. The complexity of realistic half cells with electrode, active particles, conducting carbons, binders, solvent, electrolyte and additives necessitates to introduce appropriate approximations and simplifications. According to one of these simplified approaches, the electrolyte can just be regarded as a thermodynamic reservoir which supplies particles that are characterized by their chemical potential [25, 26]. In thermal equilibrium, the appropriate thermodynamical potential describing the electrode consisting of different particles $i$ is the Gibbs free energy $G(T, p, \{N_i\})$. The most stable electrode surface structure is given by the minimum of the surface free energy that can be expressed [27] as

$$\Delta\gamma(T,p) = \frac{1}{A_s}\left(G(T,p,\{N_i\}) - \sum_i N_i\mu_i(T,p)\right) \quad (1)$$

$$\approx \frac{1}{A_s}\left(E_{\rm ads} - \sum_i N_i\Delta\mu_i(T,p)\right) \ , \quad (2)$$

where $A_s$ is the surface area. In the last line (eq. (2)), we have separated the pressure and temperature-dependent components from the chemical potential. The adsorption energy $E_{\rm ads}$ with respect to the most stable species in the reservoir in the limit of zero temperature and pressure can be derived from DFT calculations. Note that the values of $E_{\rm ads}$, $A_s$, and $N_i$ are assumed to be taken with respect to a chosen surface unit cell. Any change in entropy and zero-point energies upon adsorption can be taken into account, but in fact it is often neglected in theoretical surface studies as these contributions are typically small [27].

For electrochemical systems in the presence of an electrode potential $U$, the chemical potential $\mu$ has to be replaced by the electrochemical potential

$$\tilde{\mu} = \mu + neU \ , \quad (3)$$

where $n$ is the charge of the particle. Still the problem remains that the reservoir is given by the electrolyte which requires to derive the solvation energy of the species as the proper reference. The determination of solvation energies necessitates computationally demanding thermal integration schemes [28]. These efforts can in fact be avoided using the concept of the computational hydrogen electrode [25, 26]. It is based on the fact that often the electrode potential of redox couples or redox potential can be used to select the most convenient reference species. This is illustrated for the redox couple $\frac{1}{2}\,\mathrm{A_2} + e^- \rightleftarrows \mathrm{A^-}$ [29]. The electrochemical potential of the solvated anion is then given by

$$\tilde{\mu}(\mathrm{A^-(aq)}) - \mu(e^-) = \frac{1}{2}\mu(\mathrm{A_2(g)}) + e(U_{\rm SHE} - U^0) + k_{\rm B}T\ln a_{\mathrm{A^-}} \ , \quad (4)$$

where $U^0$ is the reduction potential of the corresponding anion with respect to the potential of the standard hydrogen electrode (SHE) and $a_{\mathrm{A^-}}$ its activity coefficient. Neglecting the change of zero-point energies and the entropy change upon adsorption, at standard conditions ($a_{\mathrm{A^-}} = 1$, pH = 0, $p = 1\,\mathrm{bar}$, $T = 298\,\mathrm{K}$) the free energy of adsorption as a function of the electrode potential is given by

$$\Delta\gamma(U_{\rm SHE}) = \frac{1}{A_s}\left(E_{\rm ads} - N_{\rm ads}e(U_{\rm SHE} - U^0)\right) \ , \quad (5)$$

where the adsorption energy $E_{\rm ads}$ is taken with respect to the molecule $\mathrm{A_2}$ in the gas phase which can usually conveniently be calculated. For other concentrations of species $A$ in the electrolyte, the corresponding electrode potential has to be shifted by $k_{\rm B}T\ln a_{\mathrm{A^-}}$. At room temperature this corresponds to about 60 meV when the activity is changed by one order of magnitude. The same applies if the pH value is changed by 1. Note that the concept of the computational hydrogen electrode is not restricted to aqueous electrolytes, also the effect of solid electrolytes might be treated within this concept as long as the definition of a chemical potential in thermal equilbrium is justified.

### B. Interfaces in electrochemical cells

We will first illustrate this approach with respect to the equilibrium coverage of halides on metal electrodes [30]. Electrochemistry is concerned with processes at the interface between an electron and an ion conductor [31], and in the case of an aqueous electrolyte the ion conductivity is mediated by solvated ions. Electrolytes used in electrocatalysis have typical ion concentrations of about 0.1 M [32] which means that for 550 water molecules there is one ion in the electrolyte. Still, the concentration of adsorbed ions, in particular *anions*, on the electrode surface is often much larger because of the strong ion-electrode interaction. For example, halide coverages on metal electrodes are of the order of 1/3 according to experiment [32]. These specifically adsorbed ions are an integral part of the electrochemical double layer [31]. At the same time, they modify the adsorption properties of

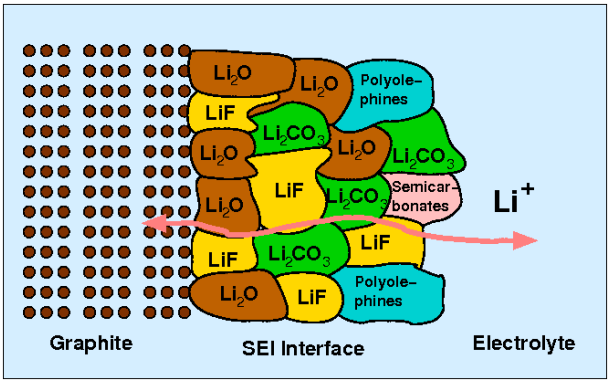


Figure 1. Schematic structure of the solid liquid interphase forming at negative battery electrodes. .

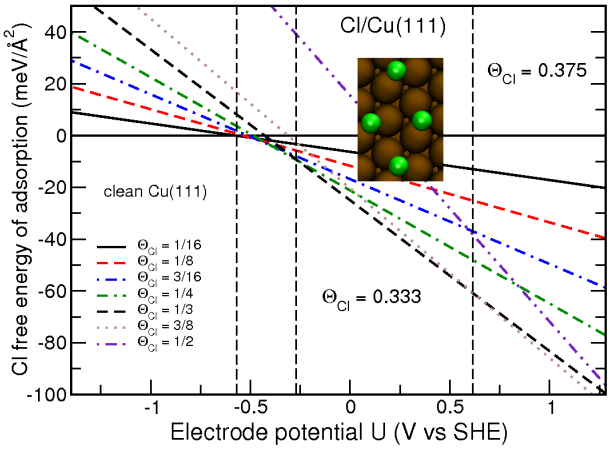


Figure 2. Calculated electrochemical equilibrium coverage of chlorine on Cu(111) at standard condition as a function of the electrode potential vs. SHE. The inset illustrates the structure of the chlorine $\sqrt{3} \times \sqrt{3}$ structure (adapted from [30]) .

the electrode substantially [33]. It is for example well-known that adsorbed chlorine reduces the adsorption energies of hydrogen and increases the reaction barrier in hydrogen dissociation [34]. Considering the importance of anion adsorption in surface electrochemistry, it is unfortunate that so far there has only been a limited number of theoretical studies addressing this issue [35, 36].

In Fig. 2, the free energy of adsorption of chlorine on Cu(111) determined according to Eq. 5 is plotted as an example. This system is well-studied experimentally with atomic resolution [32, 37, 38] and thus allows a close comparison between experiment and theoretical predictions. Furthermore, it is well-known that the presence of anions significantly influences the underpotential deposition of Cu [39]. As Fig. 2 demonstrates, in a rather large potential window above -0.3 V, the $(\sqrt{3} \times \sqrt{3})$ structure is stable which is consistent with the experiment [37, 38]. Such a high halide coverage has a significant impact on the properties of the electrode/electrolyte interface as it for example displaces water layers away from the metal surface [40].

For aqueous electrolytes, the pH value of the electrolyte plays an important role, as the concentration of protons in the electrolyte can lead to a hydrogen layer on the electrode. This is in particular true for Pt electrodes [7, 41, 42]. On Cu(111), however, no hydrogen layer is observed because of its small hydrogen adsorption energy [43]. As there is in addition a repulsive interaction between adsorbed chlorine and hydrogen which further reduces the hydrogen adsorption energy, hydrogen adsorption on Cu(111) does not need to be considered under electrochemical conditions.

It should, however, be mentioned that the presence of the electrolyte and varying electrode potentials has been entirely neglected in the determination of the adsorption energies which are the basis of the free energies of adsorption shown in Fig. 2. This represents a severe approximation, but as the consideration of the electrochemical environment is computationally rather demanding, the validity of this approximation is hard to judge at the moment.

However, it should be noted that the thermodynamic approach can be coupled with a more realistic representation of the electrochemical environment. For the determination of the adsorption energy $E_{\mathrm{ads}}$ appearing in eq. 5 the presence of the electrolyte and electric fields can be taken into account [25]. The electrolyte can be described explicitly in an atomistic model or implicitly through a polarizable medium [44]. We are currently testing an implicit solvent model [45] implemented into the VASP code and compare it results obtained with an explicit representation of an aqueous electrolyte [40]. Table I compares calculated results for standard electrode potentials in water with experimental values [46]. To obtain the reference value for the proton in solution, it has been used that at standard conditions the proton is at equilibrium with $H_2$ in the gas phase. The agreement between experiment and theory in Tab. I is quite satisfactory given the approximative nature of the computational approach.

Table I. Standard electrode potentials in water in V calculated by DFT using an implicit solvent model [45] and derived from experiment [46].

| Reaction | Theory | Experiment |
|---|---|---|
| $H^+/H_2$(aq) | −0.003 | −0.091 |
| $CH_3OH$(aq)/CO2(aq),$H^+$ | 0.263 | 0.020 |
| $CH_3OH$(aq),$H^+/CH_4$(g) | 0.694 | 0.583 |
| $O_2$(aq),$H^+/H_2O$(aq) | 1.424 | 1.272 |
| $CO_2$(g),$H^+/CH_4$(g) | 0.384 | 0.169 |

### C. Interfaces in batteries

We now illustrate this thermodynamical approach also for battery interfaces. Surfaces and surface properties of Li intercalation cathodes are typically studied by electronic structure methods without taking anything into account besides the clean surface [47–49]. Typical cathode intercalation materials are transition metal compounds (oxides/sulfates/fluorides) with admixed atomic species (Li, Na/Mg, N/F) and/or functional groups ($PO_4$, $SiO_4$) in order to stabilize the material against chemical and/or structural decomposition during delithiation. One complication arises from the fact that the behavior of strongly localized and correlated d-states of transition metal ions is typically not well described by standard DFT functionals such as LDA and GGA. Correct structural, electronic and energetic properties can only be obtained if appropriate DFT functionals are applied. A wide-spread approach is to use GGA+$U$ methods [11] where $U$ is an on-site Coulomb interaction parameter which is typically empirically determined. Furthermore, the simplest chemical structures are ternary and quaternary compounds, which relates to a variety of possible surface terminations that have to be tested to determine relevant surface structures. Though stable terminations for simple ternary compounds can often be rationalized by simple bond cutting considerations [47, 50–52] it was also shown that more complicated phenomena can be favorable such as reconstructions [53] and exchanged sites at the surface [47, 54]. Furthermore traditional classifications of the stability of ionic surfaces due to polarity become impractical for complex surfaces and more *subtle* definitions should be considered [55]. In principle also the possibility of ion exchange and non-stoichiometry needs be tested e.g. by ab-initio thermodynamics approaches [27, 56, 57].

Depending on the anisotropy of the structure, Li diffusion can be 1-, 2- or 3-dimensional rendering surfaces active or inactive upon delithiation. Binding energies, redox-potentials and hopping barriers can strongly deviate from the bulk value near surfaces and in subsurface regions [48, 58–60]. Especially for materials with 1D diffusion, the crossing of the orthogonal surface planes can have tremendous effects on the performance, and theoretical computations succeeded in correctly describing appropriate surface modifications for improved material properties[58].

We have however identified an additional difficulty in such calculations that has, to our knowledge, not been discussed and is hence unresolved. It can be illustrated by the following prototypical ab-initio thermodynamics calculations we have performed on the material $Li_2FeSiO_4$. All computational details are as in [51], in particular we used density functional theory with GGA+$U$ to calculate the dependence of surface energies of different non-stoichiometric (010) surface terminations on the chemical potential of Li. The results are plotted in Fig. 3. As common, we measure the Li chemical potential

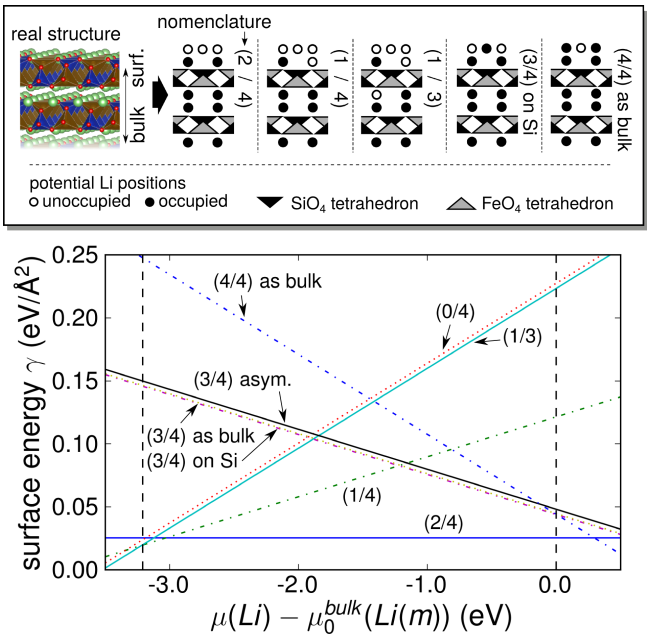


Figure 3. (010) surface composition of $Li_2FeSiO_4$ at various Li chemical potentials. The nomenclature is chosen according to the number of Li atoms per $(1 \times 1)$ unit-cell in surface and subsurface Li layers (see pictograms).

against a Li(m) electrode which allows the direct correlation of the chemical potential with the applied voltage in the cell. Hence the opposite limiting chemical potential corresponds to the delithiation voltage in this material (see vertical dashed lines in Fig. 3). Note that the potentials are derived from energy differences; thus they correspond to an open circuit situation and do not allow to estimate the dependence of the potential on the discharge rate.

Different Li compositions of surface and subsurface layers have been tested and equilibrium compositions can be determined from determining the ground-state line. Thus we find e.g. that the first Li ion per (010)-$(1 \times 1)$ unit-cell can be extracted already at a voltage of 3.03 V, which is 100 mV below the bulk delithiation potential ((1/4) in Fig. 3). Accordingly, one might speak of a reduced redox-potential or reduced binding energy of this particular Li ion.

All other calculated structures (besides the stoichiometric (2/4) termination), however, do not contribute to the ground-state line which we would naively interpret as unfavorable delithiation of surface and subsurface atoms. There are still some peculiarities about Li batteries which make the calculation of diagrams as in Fig. 3 less reliable than in the case of pure adsorption events. These are mainly related to the fact that Li battery cycling is also influencing the Li composition in the underlying bulk structure. As a result it is unclear how to assess the quality of configurational sampling as the number of possible Li configurations also in the subsurface/bulk part is impossibly large. Furthermore it is un-

clear which lattice constant should be used to simulate the structures of varying Li content as most materials expand or shrink upon delithiation. The effect on the Li chemical potentials in the case of $Li_2FeSiO_4$ is of the order of 80 meV, which has an impact on the crossing points of the lines and the limits in Fig. 3. Furthermore bulk delithiation in $Li_2FeSiO_4$ is characterized by a phase separation into $Li_2FeSiO_4$, $LiFeSiO_4$ and $FeSiO_4$ which means that the stable intermediate phase – $LiFeSiO_4$ – prevents continuous delithiation of Li atom by Li atom and induces the growth of a Li poor phase with a specific long range Li structure. For such materials the thermodynamically accessible configurational space is extremely small and thus a standard approach as discussed here by removing Li atoms in some random manner is doomed to give insignificant results. To our opinion the methodology to surface properties of these materials is still underdeveloped as even a consistent approach to study the bulk properties of such materials by ab-initio simulations does not exist yet, as shall be discussed below.

### D. Li dendrite growth in batteries

We like to draw the attention to a specific issue related to the anode side of Li-ion batteries, namely the growth of Li dendrites [61–63]. Their formation can lead to short-cuts which lead to irreversible battery damage and hazards such as battery fires. As far as pure lithium anodic batteries are concerned, additional issues such as cyclability, loss of anode material and pollution of the electrolyte by dendritic deposits become a concern [61–64]. Current theories of the dendrite formation suggest that through imperfections in the SEI, local deviations in the surface charge occur which then lead to an increased lithium deposition [65–67].

Again, the process of dendrite formation is much too complex to be addressed realistically and completely on a first-principles level. Coarse-grained models have been used to address the factors influencing Li dendrite growth [68]. The simulations have for example shown that the dendrite formation propensity increases with electrode overpotential. Interestingly enough, in contrast to Li, magnesium does not tend to form agglomerates on copper or gold substrates, but instead shows a trend to form uniform structures [69, 70]. This is gratifying as Mg is a promising candidate for substituting lithium in batteries [71, 72] as its volumetric energy density is even higher than the one of Li since Mg can carry two elementary charge units. In addition, Mg is much more abundant in the earth crust, making it also economically very attractive.

The fact that Mg in contrast to Li apparently does not exhibit dendrite growth raises the question about the differences between these two elements. In order to get a basic understanding, it is imperative to consider and contrast fundamental properties of these two metals. These issues were addressed in a recent DFT study [73] which concluded that the stronger bonding between Mg compared to Li might be decisive as the diffusion barriers of both materials are rather similar. Note that the surface structures resulting from growth are controlled by migration processes [74–76].

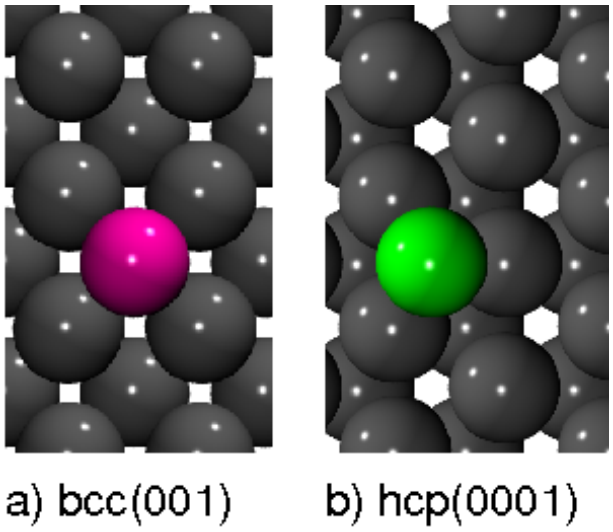


Figure 4. Structure of the most favorable surface terminations together with an adatom for bcc and hcp metals: a) bcc(001), b) hcp(0001) .

These results of the DFT study [73] were derived by considering several low-dimensional metallic structures, but the relevance of the different structures was not assessed. Here we would like to argue that it is crucial to concentrate on the energetically most favorable structures as they will be most abundant. First we address the cohesive energies of Li and Mg which are listed in Tab. II. The calculated values obtained by PBE-DFT compare favorably with those obtained in the experiment [77]. The cohesive energy of Li is slightly larger than the one of Mg. However, as far as the strength of the intermetallic interaction is concerned one has to take into account that Li is a *body-centered cubic* (bcc) metal with an eight-fold coordination whereas Mg is a *hexagonal close-packed* (hcp) metal with a twelve-fold coordination so that the energy per metal bond is stronger in Li than in Mg.

There is another characteristic difference between bcc and hcp metals. For bcc metals, typically the (001) surface termination illustrated in Fig. 4a is the most stable one, which is also true for Li [78], whereas for hcp metals like Mg it the the hexagonal close-packed (0001) surface [73] (Fig. 4b). The bcc(001) surface with its most favorable fourfold-hollow adsorption sites is more open

Table II. Cohesive energies of Li and Mg in eV/atom.

| Cohesive energies (eV/atom) | Li | Mg |
|---|---|---|
| Experiment [77] | 1.63 | 1.51 |
| PBE-DFT (this work) | 1.61 | 1.50 |

and more corrugated than the hcp(0001) surface with its threefold-hollow adsorption site so that diffusion on Li(001) is hindered to a larger extent than on Mg(0001). These considerations suggest that Li exhibits a tendency towards more open structure than Mg, which is consistent with the observation that Li shows dendrite growth, but not Mg. Furthermore, note that growth theories predict that the resulting structures do not only depend on the diffusion coefficient $D$, but also on the deposition flux $F$ [79], and it is the ratio $D/F$ that enters as the critical quantity. Thus increasing the deposition flux has the same effect as decreasing the diffusivity, namely favoring more open structures. This is consistent with the observation that dendrite growth is particularly observed at high charge rates [64]. A computational study to address these issues in more detail will soon be completed in our group.

### E. Ionic liquids as battery electrolytes

Another safety concern with respect to the current generation of Li-ion batteries is the fact that the electrolytes used today such as ethylene carbonate whose adsorption on Cu(111) is illustrated in Fig. 5a are combustible at high temperature. Ionic liquids represent a promising candidate material as alternative electrolytes [80] because of their high stability, high ionic conductivity and their low flammability. Ionic liquids are room-temperature molten salts that are characterized by weak interactions because of charge delocalization on the ions. Figure 5b depicts an 1-Ethyl-3-methylimidazolium chloride bis(trifluoromethylsulfonyl)imide ($[EMIM]^+[TFSA]^-$) ionic liquid pair on Au(111). Because of the huge number of possible combinations, computational screening can be helpful in identifying suitable candidates for battery electrolytes.

It is important to note that because of the weak interaction between the ion liquid pairs and between ion liquids and any electrode it is important to take the van der Waals interaction into account [81]. Semilocal DFT functionals typically do not reproduce this kind of dispersion interaction. Fortunately, in recent years the situation has improved significantly through the development of dispersion-corrected DFT functionals [82–84] and van der Waals functionals [85]. This is in fact in general true for the adsorption of organic molecules [86, 87], but also for a proper DFT description of aqueous electrolytes [88, 89]. The structures shown in Fig. 5 have in fact been calculated using the so-called dispersion corrected PBE-D3 approach [83]. Without taking dispersion into account, these structures would incorrectly be predicted to be very weakly bound to metal electrodes. The pure PBE adsorption energy of ethylene carbonate on Cu(111) in the configuration shown in Fig. 5a is -0.17 eV while dispersion corrections lead to an adsorption energy of -0.60 eV. The rather large adsorption height of 3.125 Å illustrated in Fig. 5a indicates that no true chemical bond between Cu(111) and ethylene carbonate is formed.

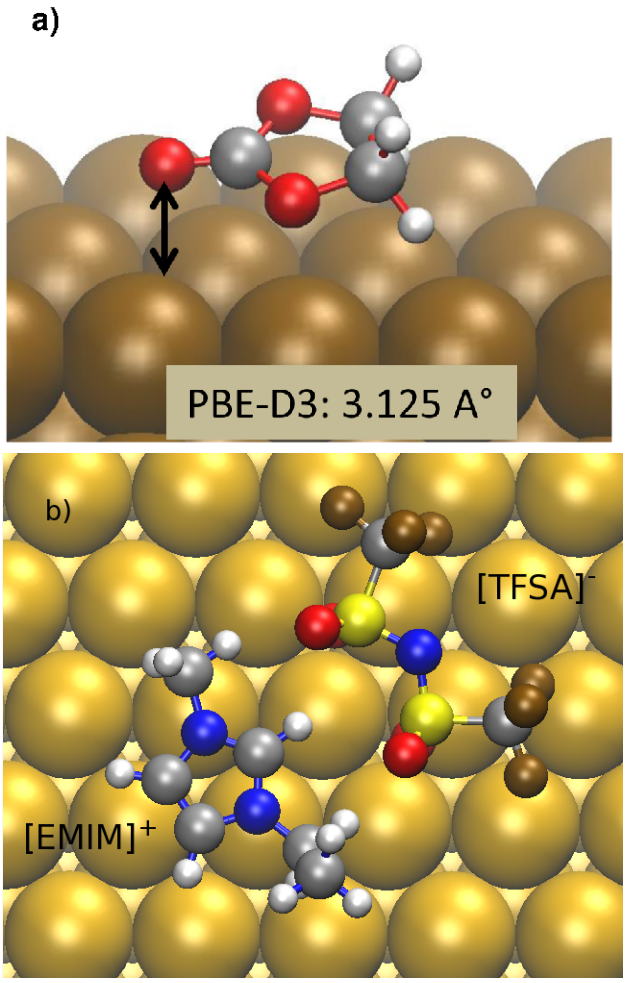


Figure 5. Calculated structures of solvent molecules on metal substrates. a) Ethylene carbonate on Cu(111), b) $[EMIM]^+[TFSA]^-$ on Au(111).

As far as the ionic liquid pair shown in Fig. 5b is concerned, the ring atoms of the EMIM cation are located 3.44 Å above the Au atoms, whereas the oxygen atoms of the TFSA anion are 2.63 Å above the surface. Both values are also indicative of the absence of a true chemical bond [86, 87]. Without dispersion corrections, the ionic liquid pair $[EMIM]^+[TFSA]^-$ hardly binds to a metal electrode (adsorption energy -0.05 eV) whereas the inclusion of dispersion corrections leads to an adsorption energy of -1.60 eV, a value close to the one found for a similar ionic liquid pair on Ag(111) [81]. The larger amount of van der Waals attraction compared to ethylene carbonate is mainly due to the larger size of the ionic liquid pair.

## IV. BULK VOLUME CHANGES

In order to understand and model the de-/lithiation processes of the active electrode particles, it is firstly necessary to understand the thermodynamic equilibrium properties of the active materials as the dynamic processes are the response of the system to a deviation from thermodynamic equilibrium, driven e.g. by the external voltage.

As mentioned before, even today theoretical modeling of battery materials is still separated into an atomistic and a continuum approach, as it is a classical multi-scale problem. On the one hand a continuum description of the system by some energy functional resembling the Cahn-Hilliard formulation can be applied where appropriate terms are included to pay respect to comparably large structures such as interfaces, surfaces and strain [90–92]. Such approaches can correctly include all relevant terms necessary for the phenomenological description of intercalation processes. The unknown parameters however are typically determined from experiment as it is still unclear how to consistently transfer results obtained e.g. in atomic scale ab-initio calculations.

On the other hand computationally expensive thermodynamic averaging of atomistic Hamiltonians can be performed by parametrizing an analytic function (e.g. a cluster expansion) according to ab-initio determined energies for different Li configurations [93–97]. As this is rather time consuming such approaches have to our knowledge only be applied to general thermodynamic properties, such as bulk phase diagrams which e.g. determine whether a material reacts via a single or two phase pathway. Those two reaction mechanisms differ specifically as in the former case deintercalation can be driven by the least overpotential, whereas in the second case a certain overpotential threshold needs to be exceeded to drive the reaction, as the creation of phase boundaries as well as strain induce a certain energy barrier absent in single phase reactions. This fact causes one of the main drawbacks of such "pure" ab-initio approaches: due to the limited number of atoms and the reduced computational cell, long range elastic contributions cannot be captured, or are included only effectively in an uncontrolled way. Many publications in recent years have however shown that strain has a major effect on the thermodynamics of phase separating intercalation compounds[98–101]. Therefore an exclusive description of such materials based on an atomistic picture that only captures short range interactions is expected to be at least incomplete. This is especially relevant for the description of phase-separating intercalation compounds ($LiFePO_4$, $Li_2FeSiO_4$) and high energy battery concepts such as conversion batteries [102] and beyond [9, 103].

Consistent coarse graining approaches to bridge the gap between the discrete description and the continuum counterpart are still missing. Thus in our opinion one major challenge in ab-initio simulations of battery materials is to resolve the interdependence of long-range continuum solutions that depend on the atomistically determined parameters, maybe in a self-consistent-like manner.

In our group we have recently developed a first step to do so, namely by modeling the initial steps of deintercalation in a phase separating compound by parametrizing a continuum two phase model from density functional theory calculations (DFT) in a consistent way. Details will be published elsewhere, first results however indicate that delithiation kinetics in $Li_2FeSiO_4$ is strongly enhanced by nucleation at wetted surfaces.

## V. CONCLUSIONS

First-principles electronic structure calculations are a powerful tool to elucidate microscopic details of structures and processes occurring at the interface between an ion and an electron conductor in electrochemical energy storage and conversion devices. Still, electrochemical systems represent a challenge for electronic structure methods because of the complexity of the interfaces requiring statistical mechanical and thermodynamical considerations, the presence of charged systems and electric fields, and the wide range of interactions from strong correlations inside the electrode to weak dispersion forces in the electrolyte. However, as demonstrated in this paper there are approaches available to address these issues.

As a starting point we demonstrated the success of traditional ab-initio surface thermodynamics approaches for aqueous electrochemical systems. The main effect of the electrolyte can be included to some extent by a polarizable continuum which avoids time consuming statistical averages. Furthermore ab-initio techniques enabled us to study material specific behavior such as dendrite growth at a much lower degree of complexity than the real system. Still it is important to understand the true influence of the electrode-electrolyte interaction. However, the proper description of the substrate-adsorbate interaction by common exchange correlation functionals is still a challenge. Note also that mainly structural information has so far been addressed by first-principles studies, as the modeling of processes such as charging/discharging or passivation requires the determination of transformation mechanisms which can be rather demanding.

Modeling intercalation electrodes is even a more difficult task as particle exchange with subsurface layers needs to be considered in addition to adsorption-like processes. The sheer number of surface and subsurface terminations requires tremendous configurational scanning efforts. Furthermore, the fact that battery cycling affects strongly the underlying bulk structure neccessitates a proper understanding of the bulk behavior in contrast to the traditional surface thermodynamics approach. This however is is rather challenging as it requires multiscale techniques, and the methodology will probably only be developped in the years to come.

On a fundamental level, we like to add the following

remark. On the one hand, it is true that the advantage of simulations is that there is a full control of the studied system. This allows a detailed analysis and interpretation of the computational results. On the other hand, since any modeling involves approximations, it is necessary to validate the model used to simulate a system, and this can best be done when a direct comparison between experimental and theoretical data is possible. Unfortunately, the experimental in-situ elucidation of processes in electrochemical systems is not trivial because of their complexity. Thus sometimes the relevance of a theoretical study is hard to assess. Therefore, the progress in the first-principles modeling of structures and processes in electrochemical energy storage and transfer is strongly linked to the advances in experimental techniques, and it requires a close collaboration between theory and experiment.

## ACKNOWLEDGMENTS

Computer time has been provided by the BW-Grid of the federal state of Baden-Württemberg/Germany. Useful discussions with Wolfgang Schmickler and Eckhard Spohr are gratefully acknowledged. Partial funding has been provided by the German Science Foundation through contracts GR 1503/21-2, 22-2, and 25-1.

[1] J. Goodenough, J. Solid State Electrochem. **16** (2012) 2019.
[2] E. Spohr, Electrochim. Acta **49** (2003) 23 .
[3] C. Hartnig and M. T. M. Koper, J. Phys. Chem. B **108** (2004) 3824.
[4] C. D. Taylor, S. A. Wasileski, J.-S. Filhol, and M. Neurock, Phys. Rev. B **73** (2006) 165402.
[5] E. Skúlason, G. S. Karlberg, J. Rossmeisl, T. Bligaard, J. Greeley, H. Jónsson, and J. K. Nørskov, Phys. Chem. Chem. Phys. **9** (2007) 3241.
[6] S. Schnur and A. Groß, New J. Phys. **11** (2009) 125003.
[7] S. Schnur and A. Groß, Catal. Today **165** (2011) 129.
[8] N. Bonnet, T. Morishita, O. Sugino, and M. Otani, Phys. Rev. Lett. **109** (2012) 266101.
[9] J. Maier, Angew. Chem. Int. Ed. **52** (2013) 4998.
[10] A. Groß, Surf. Sci. **500** (2002) 347.
[11] M. S. Islam and C. A. J. Fisher, Chem. Soc. Rev. **43** (2014) 185.
[12] J. K. Nørskov, F. Abild-Pedersen, F. Studt, and T. Bligaard, Proc. Natl. Acad. Sci. **108** (2011) 937.
[13] G. Kresse and J. Furthmüller, Phys. Rev. B **54** (1996) 11169.
[14] P. E. Blöchl, Phys. Rev. B **50** (1994) 17953.
[15] G. Kresse and D. Joubert, Phys. Rev. B **59** (1999) 1758.
[16] J. P. Perdew, K. Burke, and M. Ernzerhof, Phys. Rev. Lett. **77** (1996) 3865.
[17] K. Leung and J. L. Budzien, Phys. Chem. Chem. Phys. **12** (2010) 6583.
[18] K. Leung and C. M. Tenney, J. Phys. Chem. C **117** (2013) 24224.
[19] K. Ushirogata, K. Sodeyama, Y. Okuno, and Y. Tateyama, J. Am. Chem. Soc. **135** (2013) 11967.
[20] Y. Ma and P. B. Balbuena, J. Electrochem. Soc. **161** (2014) E3097.
[21] M. E. Spahr, H. Buqa, A. Wüursig, D. Goers, L. Hardwick, P. Novak, F. Krumeich, J. Dentzer, and C. Vix-Guterl, J. Power Sources **153** (2006) 300 .
[22] O. Borodin, G. D. Smith, and P. Fan, J. Phys. Chem. B **110** (2006) 22773.
[23] O. Borodin, G. V. Zhuang, P. N. Ross, and K. Xu, J. Phys. Chem. C **117** (2013) 7433.
[24] M. E. Björketun, Z. Zeng, R. Ahmed, V. Tripkovic, K. S. Thygesen, and J. Rossmeisl, Chem. Phys. Lett. **555** (2013) 145 .
[25] J. K. Nørskov, J. Rossmeisl, A. Logadottir, L. Lindqvist, J. R. Kitchin, T. Bligaard, and H. Jónsson, J. Phys. Chem. B **108** (2004) 17886.
[26] J. K. Nørskov, T. Bligaard, A. Logadottir, J. R. Kitchin, J. G. Chen, S. Pandelov, and U. Stimming, J. Electrochem. Soc. **152** (2005) J23.
[27] K. Reuter and M. Scheffler, Phys. Rev. B **65** (2001) 035406.
[28] A. R. Leach, *Molecular Modelling: Principles and Applications*, Pearson, Harlow, 2nd edition, 2001.
[29] H. A. Hansen, I. C. Man, F. Studt, F. Abild-Pedersen, T. Bligaard, and J. Rossmeisl, Phys. Chem. Chem. Phys. **12** (2010) 283.
[30] F. Gossenberger, T. Roman, and A. Groß, Surf. Sci. (2014) doi: 10.1016/j.susc.2014.01.021.
[31] W. Schmickler and E. Santos, *Interfacial Electrochemistry*, Springer, Berlin, 2nd edition, 2010.
[32] O. M. Magnussen, Chem. Rev. **107** (2002) 679.
[33] D. V. Tripkovic, D. Strmcnik, D. van der Vliet, V. Stamenkovic, and N. M. Markovic, Faraday Discuss. **140** (2009) 25.
[34] A. Groß, Surf. Sci. **608** (2013) 249 .
[35] K.-Y. Yeh, N. A. Restaino, M. R. Esopi, J. K. Maranas, and M. J. Janik, Catal. Today **202** (2013) 20 .
[36] A. Comas-Vives, J. Bandlow, and T. Jacob, Phys. Chem. Chem. Phys. **15** (2013) 992.
[37] M. Kruft, B. Wohlmann, C. Stuhlmann, and K. Wandelt, Surf. Sci. **377-379** (1997) 601.
[38] P. Broekmann, M. Wilms, M. Kruft, C. Stuhlmann, and K. Wandelt, J. Electroanal. Chem. **467** (1999) 307.
[39] N. Markovic and P. N. Ross, Langmuir **9** (1993) 580.
[40] A. Groß, F. Gossenberger, X. Lin, M. Naderian, S. Sakong, and T. Roman, J. Electrochem. Soc. **161** (2014) E3015 .
[41] N. M. Marković and P. N. Ross Jr., Surf. Sci. Rep. **45** (2002) 117.
[42] T. Roman and A. Groß, Catal. Today **202** (2013) 183.
[43] S. Sakong and A. Groß, Surf. Sci. **525** (2003) 107.
[44] A. Klamt, J. Phys. Chem. **99** (1995) 2224.
[45] K. Mathew, R. Sundararaman, K. Letchworth-Weaver, T. A. Arias, and R. G. Hennig, J. Chem. Phys. **140** (2014) 084106.
[46] S. G. Bratsch, J. Phys. Chem. Ref. Data **18** (1989) 1.

[47] L. Wang, F. Zhou, Y. S. Meng, and G. Ceder, Phys. Rev. B **76** (2007) 165435.

[48] L. Wang, F. Zhou, and G. Ceder, Electrochem. Solid-State Lett. **11** (2008) A94.

[49] L. Daheron, H. Martinez, R. Dedryvere, I. Baraille, M. Menetrier, C. Denage, C. Delmas, and D. Gonbeau, J. Phys. Chem. C **113** (2009) 5843.

[50] R. Benedek and M. M. Thackeray, Phys. Rev. B **83** (2011) 195439.

[51] N. Hörmann and A. Groß, J. Solid State Electrochem. **18** (2014) 1401.

[52] Y. Kim, H. Lee, and S. Kang, J. Mater. Chem. **12** (2012) 12874.

[53] C. Y. Ouyang, Ž. Šljivančanin, and A. Baldereschi, J. Chem. Phys. **133** (2010) 204701.

[54] A. Karim, S. Fosse, and K. A. Persson, Phys. Rev. B **87** (2013) 075322.

[55] N. Hörmann and A. Groß, ChemPhysChem **15** (2014) 2058.

[56] D. Kramer and G. Ceder, Chem. Mater. **21** (2009) 3799.

[57] K. A. Persson, B. Waldwick, P. Lazic, and G. Ceder, Phys. Rev. B **85** (2012) 235438.

[58] K.-S. Park, P. Xiao, S.-Y. Kim, A. Dylla, Y.-M. Choi, G. Henkelman, K. J. Stevenson, and J. B. Goodenough, Chem. Mater. **24** (2012) 3212.

[59] D. Qian, Y. Hinuma, H. Chen, L.-S. Du, K. J. Carroll, G. Ceder, C. P. Grey, and Y. S. Meng, J. Am. Chem. Soc. **134** (2012) 6096.

[60] D. A. Tompsett, S. C. Parker, P. G. Bruce, and M. S. Islam, Chem. Mater. **25** (2013) 536.

[61] W.-S. Kim and W.-Y. Yoon, Electrochim. Acta **50** (2004) 541.

[62] K. Nishikawa, T. Mori, T. Nishida, Y. Fukunaka, M. Rosso, and T. Homma, J. Electrochem. Soc. **157** (2010) A1212.

[63] G. Girishkumar, B. McCloskey, A. C. Luntz, S. Swanson, and W. Wilcke, J. Phys. Chem. Lett. **1** (2010) 2193.

[64] K. Xu, Chem. Rev. **104** (2004) 4303.

[65] A. Schechter and D. Aurbach, Langmuir **15** (1999) 3334.

[66] Y. S. Cohen, Y. Cohen, and D. Aurbach, J. Phys. Chem. B **104** (2000) 12282.

[67] J. Christensen, P. Albertus, R. S. Sanchez-Carrera, T. Lohmann, B. Kozinsky, R. Liedtke, J. Ahmed, and A. Kojic, J. Electrochem. Soc. **159** (2011) R1.

[68] M. Z. Mayers, J. W. Kaminski, and T. F. Miller, J. Phys. Chem. C **116** (2012) 26214.

[69] Q. S. Zhao and J. L. Wang, Electrochim. Acta **56** (2011) 6530.

[70] D. Aurbach, Y. Cohen, and M. Moshkovich, Electrochem. Solid-State Lett. **4** (2001) A113.

[71] P. Novak, R. Imhof, and O. Haas, Electrochim. Acta **45** (1999) 351.

[72] H. D. Yoo, I. Shterenberg, Y. Gofer, G. Gershinsky, N. Pour, and D. Aurbach, Energy Environ. Sci. **6** (2013) 2265.

[73] C. Ling, D. Banerjee, and M. Matsui, Electrochim. Acta **76** (2012) 270 .

[74] T. Michely, M. Hohage, M. Bott, and G. Comsa, Phys. Rev. Lett. **70** (1993) 3943.

[75] P. Ruggerone, A. Kley, and M. Scheffler, Prog. Surf. Sci. **54** (1997) 331.

[76] X. Lin, A. Dasgupta, F. Xie, T. Schimmel, F. Evers, and A. Groß, Electrochim. Acta **140** (2014) 505.

[77] C. Kittel, *Introduction to Solid State Physics*, John Wiley & Sons, New York, eigth edition, 2004.

[78] K. Doll, N. M. Harrison, and V. R. Saunders, J. Phys.: Condens. Matter **11** (1999) 5007.

[79] J. A. Venables, Phys. Rev. B **36** (1987) 4153.

[80] M. Armand, F. Endres, D. R. MacFarlane, H. Ohno, and B. Scrosati, Nature Mater. **8** (2009) 621.

[81] F. Buchner, K. Forster-Tonigold, B. Uhl, D. Alwast, N. Wagner, H. Farkhondeh, A. Groß, and R. J. Behm, ACS Nano **7** (2013) 7773.

[82] S. Grimme, J. Comput. Chem. **25** (2004) 1463.

[83] S. Grimme, J. Antony, S. Ehrlich, and H. Krieg, J. Chem. Phys. **132** (2010) 154104.

[84] A. Tkatchenko and M. Scheffler, Phys. Rev. Lett. **102** (2009) 073005.

[85] M. Dion, H. Rydberg, E. Schröder, D. C. Langreth, and B. I. Lundqvist, Phys. Rev. Lett. **92** (2004) 246401.

[86] K. Tonigold and A. Groß, J. Chem. Phys. **132** (2010) 224701.

[87] J. Carrasco, J. Klimes, and A. Michaelides, J. Chem. Phys. **138** (2013) 024708.

[88] K. Tonigold and A. Groß, J. Comput. Chem. **33** (2012) 695.

[89] K. Forster-Tonigold and A. Groß, J. Chem. Phys. **141** (2014) 064501.

[90] D. Burch and M. Z. Bazant, Nano Lett. **9** (2009) 3795.

[91] D. A. Cogswell and M. Z. Bazant, ACS Nano **6** (2012) 2215.

[92] D. A. Cogswell and M. Z. Bazant, Nano Lett. **13** (2013) 3036.

[93] G. Ceder, Comput. Mater. Sci. **1** (1993) 144 .

[94] A. V. der Ven, J. Thomas, Q. Xu, and J. Bhattacharya, Math. Comput. Simulat. **80** (2010) 1393 .

[95] R. Malik, F. Zhou, and G. Ceder, Nature Mater. **10** (2011) 587.

[96] K. Persson, Y. Hinuma, Y. S. Meng, A. Van der Ven, and G. Ceder, Phys. Rev. B **82** (2010) 125416.

[97] E. Lee and K. A. Persson, Chem. Mater. **25** (2013) 2885.

[98] G. Chen, X. Song, and T. J. Richardson, Electrochem. Solid-State Lett. **9** (2006) A295.

[99] N. Meethong, H.-Y. Huang, S. Speakman, W. Carter, and Y.-M. Chiang, Adv. Funct. Mater. **17** (2007) 1115.

[100] A. Van der Ven, K. Garikipati, S. Kim, and M. Wagemaker, J. Electrochem. Soc. **156** (2009) A949.

[101] M. Wagemaker, F. M. Mulder, and A. Van der Ven, Advanced Materials **21** (2009) 2703.

[102] F. Lin, I. M. Markus, D. Nordlund, T.-C. Weng, M. D. Asta, H. L. Xin, and M. M. Doeff, Nat. Commun. **5** (2014) 3529.

[103] J. Maier, Nature Mater. **4** (2005) 805.